Preprints of the 18th IFAC World Congress
Milano (Italy) August 28 - September 2, 2011

An Improved Multivariate Image Analysis Method for Quality Control of Nanofiber Membranes

Pierantonio Facco * **Andrea Masiero** ** **Fabrizio Bezzo** *
Alessandro Beghi ** **Massimiliano Barolo** *

* *Dipartimento di Principi e Impianti di Ingegneria Chimica, Università di Padova, via Marzolo 9, 35131 Padova, Italy. (e-mail: pierantonio.facco@ unipd.it)*
** *Dipartimento di Ingegneria dell'Informazione, Università di Padova, via Gradenigo 6/B, 35131 Padova, Italy, (e-mail: masiero@dei.unipd.it)*

Statistical quality monitoring; Multivariate image analysis; Texture analysis; PLS; Wavelet ; Image recognition; Classification; Image processing; Image analysis; Fast Fourier transforms.

Abstract: Multivariate image analysis is a widely used technique for computing a spatial statistical characterization of an image. In this paper a modified method for multivariate image analysis is presented. The proposed method reformulates the approach previously presented by Bharati et al. [2004] extending its range of applicability by reducing its computational complexity and its memory requirements: this allows to take into consideration a larger set of spatial statistics to characterize the image texture. The proposed approach is applied to a case study concerning the estimation of the fiber diameter distribution in nanostructured membranes. The results suggest that the optimum range of spatial statistics used for characterizing the image is related to the size of the main textural features.

1. INTRODUCTION

The quality of several materials is determined by surface characteristics (like regularity, roughness, coarseness, presence of pits or scratches, and so on), which may be relevant at the visible level or at a microscopic scale. When these surface attributes are encoded into digital images, they are associated to the variation of intensity levels between pixels belonging to a given neighborhood, i.e. to a spatial form of information known as texture. Quality monitoring by automated visual inspection systems based on on-line or off-line image texture analysis has tremendously expanded in the last few years (Liu and MacGregor [2007]), due to the increased availability of inexpensive digital cameras and computing power. Several areas have benefited from this expansion, ranging from product processing/manufacturing (Liu et al. [2005b], Facco et al. [2009], Liu et al. [2005a]), to medical, pharmaceutical, and forensic sciences (Garcia-Munoz and Gierer [2010], Kucheryavski et al. [2009]).

Bharati et al. [2004] provide a review of image texture analysis methods for product quality monitoring. They also show that using multivariate statistical tools, like principal component analysis (PCA; Jackson [1991]) or projection to latent structures (PLS; Geladi and Kowalski [1986]), to extract textural properties directly from a digital image is ineffective because of the loss of spatial information that an image is subject to after being unfolded. To overcome this problem, they propose a very effective way to regain spatial information by augmenting the image with shifted versions of itself (i.e. by applying different spatial filters to the image), in such a way that the spatial information associated to each pixel is captured by linking the pixel intensity to that of neighboring pixels. By proceeding this way, a truly multivariate intensity dataset can be built from the shifted and unfolded images in the form of a 2-D matrix, and spatial features can be easily extracted from this matrix using PCA or PLS. This approach has proved to be very effective in several applications, e.g. quality monitoring of paper transformation (Reis and Bauer [2009]) and of ceramic tile (Prats-Montalban and Ferrer [2007]).

However, one drawback of this approach is that the selected dimension of the neighborhood, wherein the original image is shifted, directly affects the multivariate image analysis (MIA) computation time. Therefore, when the neighboring region to be investigated is larger than say 3×3 pixels and the pixel dimension of the original image is not small, the 2-D matrix resulting from the shifting and unfolding operations may have very large column and row dimensions, giving rise to a tremendous calculation challenge for the application of MIA. Whereas in most cases analyzing a small (i.e. 3×3) neighboring region may be enough for capturing the most significant textural attributes of a surface, texture analysis may be improved in some instances if larger neighborhoods are explored.

The purpose of this paper is to augment the method of Bharati et al. [2004] by allowing much larger pixel neighborhoods to be analyzed with very low computa-

tional effort. The proposed method reformulates the MIA approach proposed by Bharati et al. [2004] in a three step procedure: first the image spatial correlations are efficiently computed by means of the fast Fourier transform (FFT) and the convolution theorem (Oppenheim and Schafer [1975]). Then, a set of spatial filters are obtained from the singular value decomposition of a, typically small, matrix of image local correlations. These filters extract the most important spatial features of the image. After that, a small set of texture descriptors is computed to summarize the statistical characteristics of the extracted features. To ensure a complete characterization of the image texture such descriptors are computed at multiple scales of resolution, using a wavelet multi-resolution representation (Mallat [1999]) of the spatial feature values. The proposed approach, in combination with a PLS model, is tested for the problem of fiber diameter characterization in nanofiber membranes.

2. NANOFIBER MEMBRANE FABRICATION

Polymer nanofiber membranes are the material considered as a case study in this work. These membranes are interesting for a wide range of industrial applications (e.g. filtration, reinforced materials, tissue engineering) and are fabricated by electrospinning, a technique exploiting an electric field to obtain nanofibers by pumping a polymer solution through a spinnerette (Rutledge and Fridrikh [2007]; Roso et al. [2008]). Figure 1 shows an example of nanofiber membrane.

In this study we would like to estimate the nanofiber diameter distribution using digital images of the membranes. The estimation technique proposed by Facco et al. [2010] is used, where textural features are extracted from a multiresolution version of the image in the form of statistical descriptors, which are then used as regressors to determine the required response (namely, the vigintiles of the nanofiber diameter distribution).

Whereas Facco et al. [2010] employed a 3×3 pixel neighborhood to build a multivariate image of the membranes under study, here we test whether exploring larger neighborhoods may prove more effective for the extraction of textural features. The results in terms of predicted fiber diameter distribution will be compared to those coming from the direct measurement of this distribution by means of the algorithm developed by Tomba et al. [2010].

3. ESTIMATION OF FIBER DIAMETER DISTRIBUTION

In this section the problem of estimating the distribution of membrane fiber diameters from a scanning electron microscope (SEM) image is decomposed in a four-step procedure:

- Image preprocessing: adjustment and denoising.
- MIA: it is applied to extract proper spatial features of the membrane fibers.
- Membrane texture characterization: a proper set of statistical descriptors is computed at multiple resolutions of the feature space obtained by means of MIA.

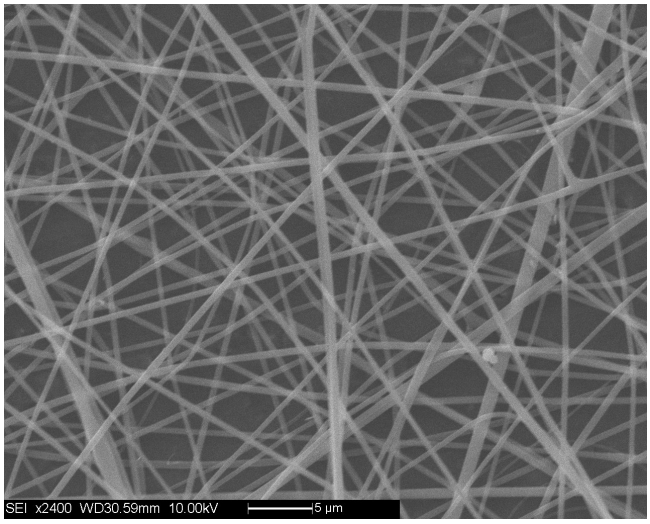

Fig. 1. Example of nanofiber membrane.

- Diameter distribution estimation: PLS is used to estimate the relation between the estimated texture descriptors and the fiber diameter distribution.

A detailed description of the four steps of such procedure will be provided in the following subsections.

3.1 Image preprocessing

Since often the SEM image is quite noisy, the first step of the procedure is a wavelet-based denoising. Furthermore, to ensure the independence of the procedure on variations of the overall image intensities, also a standard intensity equalization is applied to the image.

3.2 Multivariate image analysis

The aim of MIA is that of using a properly chosen set of spatial filters to extract the spatial features characterizing the image texture. The set of spatial filters is tailored on the data itself, i.e. they are chosen as the most representative of the second order spatial statistics of the image.

In the first part of this subsection, standard MIA method, as proposed in Bharati et al. [2004], is reviewed. Unfortunately, because of its quite high memory requirement and computational cost, in practical applications such method is restricted to consider only very small neighborhood of spatial statistics. Since texture can be characterized by statistics at quite large spatial distances (Section 4, and Idrissa and Acheroy [2002]), then in the second part of this subsection the MIA method is revised and reformulated in such a way as to allow taking into consideration also statistics on large spatial neighborhood.

Let I be the original image and I_{ij} its version shifted by i and j pixels respectively on the horizontal and vertical directions. Without loss of generality, assume that such images, $\{I_{ij}\}$, are all of the same size $r \times c$, i.e. they have been properly cropped. Furthermore, let d be the maximum distance at which the texture spatial statistics are relevant for the membrane surface characterization. Then, the MIA method (Bharati et al. [2004]) can be summarized as follows:

- Collect the $(2d+1)^2$ shifted and cropped versions I_{ij} of I, for $-d \leq i \leq d$, $-d \leq j \leq d$.
- Define the column vector Y_{ij} as the vectorization of I_{ij}, $Y_{ij} = \text{vect}(I_{ij})$. Choose a sorting order for the vectors $\{Y_{ij}\}$, then, with a slight abuse of notation, hereafter such vectors will be indicated as $Y_1, \ldots, Y_{(2d+1)^2}$.
- Form the matrix Y stacking the image vectors:
$$Y = \left[Y_1 \; Y_2 \; \ldots \; Y_{(2d+1)^2} \right] .$$
- Using Singular Value Decomposition (SVD), compute the PCA representation of Y, retaining only the n components with larger singular values ($n \leq (2d+1)^2$, but usually $n \ll (2d+1)^2$):
$$Y = USV^\top \approx XF^\top,$$
where
$S = \text{diag}(\sigma_1^2, \ldots, \sigma_{(2d+1)^2}^2)$, $\sigma_1 \geq \sigma_2 \geq \cdots \geq \sigma_{(2d+1)^2}$,
and
$$US = \left[X \mid X^\perp \right] \text{ and } V = \left[F \mid F^\perp \right] .$$

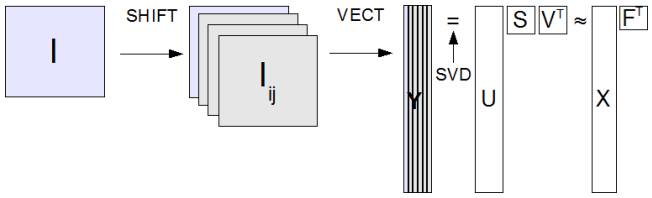

Fig. 2. MIA scheme (Bharati et al. [2004]).

Notice that the columns of F are the vectorization of n spatial filters, $f_1, f_2 \ldots f_n$, of size $(2d+1) \times (2d+1)$. Such filters are tailored on the particular spatial correlations of I: since $\{f_i\}$ are chosen between the eigenvectors of $Y^\top Y$ (Horn and Johnson [1985]) and Y contains the locally shifted versions of I (see Fig. 3), then it can be proved that F is the most representative local spatial basis for the image with respect to its local spatial correlations, i.e. the basis which allows the local representation with lowest Frobenius error when $1 \leq n < (2d+1)^2$. In this sense the computed filters can be called the most descriptive of the texture characteristics.

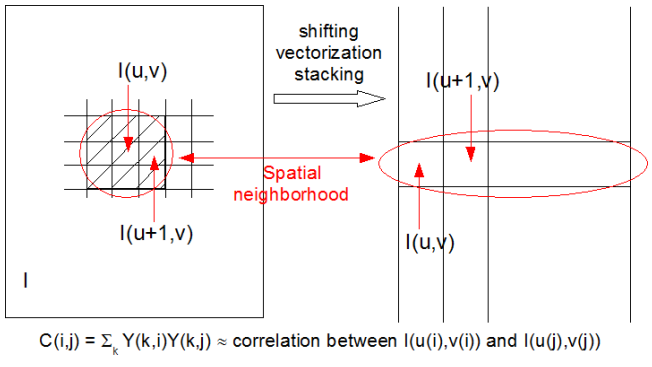

Fig. 3. Each element in C is related to the spatial correlation between two points, $(u(i), v(i))$ and $(u(j), v(j))$, in I, where $u(\cdot)$ and $v(\cdot)$ are functions which associate a column index in Y to a proper spatial position in I.

Then, f_i is a spatial feature extractor: the i-th column in X, X_i, is a vector of coefficients for the spatial feature associated to f_i. Let χ_i be obtained reshaping X_i to an $r \times c$ matrix (i.e. inverting the vectorization operator). Then $\chi_i(u, v)$ is the response of f_i applied at (u, v) in I.

Y is an $(rc) \times (2d+1)^2$ matrix, where nowadays typically $r \geq 1000$ and $c \geq 1000$. Since Y can be a very large matrix, computing the SVD of Y becomes quickly unfeasible [1] as far as d becomes large, e.g. for $d \geq 3$. While in some applications small spatial filters, $d \leq 2$, can be sufficient to obtain a satisfactory characterization of the image texture, in some other cases a larger d can be necessary, e.g. see Section 4.

In the following the MIA method will be reformulated, using parsimonious (from the point of view of memory and time requirements) techniques to compute X and F.

According to the observations above, the filters can be computed as the eigenvectors of $C = Y^\top Y$: since C is a $(2d+1)^2 \times (2d+1)^2$ matrix, for the values of typical interest for d, e.g. $d \approx 10$, this computation is very fast with respect to computing the SVD of Y.

By construction C is a matrix containing the local spatial correlations of I, as shown in Fig.3. Hence, by the convolution theorem, the spatial correlations of I can be computed efficiently using the FFT, and C can be obtained properly selecting and rearranging the computed spatial correlations of I.

Furthermore, X can be computed in $O(rcnd^2)$ (where d is usually much lower than r and c), filtering the image with the spatial filters $f_1, \ldots, f_n$.

Hence, F and X can be conveniently computed as follows (improved MIA):

- Compute the spatial correlations of I using the FFT (convolution theorem).
- Rearrange the obtained correlations to form C.
- Compute $C = VS^2V^T$ via SVD.
- Set F as the first n columns of V, and compute X filtering I with the filters in F.

A more detailed comparison between the computational complexity of the MIA and its improved version will be reported in the discussion of section 4.

3.3 Multiresolution texture characterization

As described previously, each spatial filter f_i is used to extract the corresponding spatial features X_i. Since, these filters are the most descriptive for the local spatial texture statistics, they extract very representative spatial features of the texture itself. Then, this subsection aims at computing a small set of parameters statistically characterizing the texture features extracted from the spatial filters. Furthermore, since the texture can have very important and discriminative characteristics at different scales, then such characterizing parameters are computed at different resolutions.

First, a multiresolution representation of each χ_i is obtained by means of the discrete wavelet transform (DWT, Mallat [1999]). To be more precise, the Daubechies D8 wavelet has been used to compute the DWT.

[1] Because of memory and computational time requirements.

Let χ_i^j be the low-pass representation of χ_i at scale j, where $\chi_i^0 = \chi_i$. Furthermore, let p_{ij} be an histogram formed by the values in χ_i^j. In simulations of section 4 the number of bins in p_{ij} is set to 16 and they are uniformly distributed among the values assumed by χ_i^j. Without loss of generality, p_{ij} is assumed to be normalized, i.e. $\sum_h p_{ij}(h) = 1$. Then, the following statistical descriptors are computed to statistically characterize χ_i^j, $1 \leq i \leq n$, $0 \leq j \leq \bar{j}$:

$$\text{entropy}_{ij} = -\sum_h p_{ij}(h) \log_2 p_{ij}(h) \tag{1}$$

$$\text{energy}_{ij} = \|\chi_i^j\|_F \tag{2}$$

$$\text{standard dev}_{ij} = \sigma_{ij} = \sqrt{\frac{\sum_{u,v} \left(\chi_i^j(u,v) - \mu_{ij}\right)^2}{|\chi_i^j|}} \tag{3}$$

$$\text{skewness}_{ij} = \frac{\sum_{u,v} \left(\chi_i^j(u,v) - \mu_{ij}\right)^3}{|\chi_i^j| \sigma_{ij}^3} \tag{4}$$

$$\text{kurtosis}_{ij} = \frac{\sum_{u,v} \left(\chi_i^j(u,v) - \mu_{ij}\right)^4}{|\chi_i^j| \sigma_{ij}^4} - 3 \ , \tag{5}$$

where "standard dev" in (3) stands for standard deviation, $\|\cdot\|_F$ is the Frobenius norm, μ_{ij} is the sample mean of the coefficient values in χ_i^j, $|\chi_i^j|$ is the cardinality of χ_i^j, and $\bar{j}$ is a design parameter which determines how many scales have to be considered. An automatic procedure for the choice of $\bar{j}$ has been proposed by Tomba et al. [2010].

3.4 Fiber diameter estimation: PLS approach

The responses of spatial filters $\{f_i\}$ provide information about characteristic features in the image, e.g. edges, contours. Then, filter responses include also information about fiber diameters in the image. The rationale of this subsection is that of modeling the relation between the texture statistical descriptors (1)-(5) (which summarize the information provided by filter responses) and the distribution of fiber's diameters with the linear system (6). Finally, the paramenters in system (6) are computed using PLS.

Assume that T images are available during the learning procedure, where each of such images contains some dozens of fibers. Then, the diameter of these fibers can be measured numerically (Tomba et al. [2010]), although this way be computationally intensive. In particular, to increase the robustness in such estimation, the fiber diameter distribution is estimated only at its vigintiles. Then, the aim of PLS is that of estimating the relation between the texture descriptors (1)-(5) and the fiber diameter values at all the vigintiles. The estimation operation is computationally inexpensive.

Let x_t be a row vector associated to the tth learning image formed by the descriptors in (1)-(5) computed for $1 \leq i \leq n$, $0 \leq j \leq \bar{j}$. Similarly, let y_t be a row vector of length 19, where the hth element in y_t ($1 \leq h \leq 19$) is defined as follows:

$$y_t(h) = \text{value of fiber diameter at the } (5h)\text{th percentile in image } t.$$

Then, PLS is used to compute a linear regression between the x_t and the y_t vectors:

$$\begin{cases} x_t = z_t P^\top + e_t \\ y_t = z_t Q^\top + \eta_t \end{cases} , \ 1 \leq t \leq T \ , \tag{6}$$

where P and Q are model matrices to be learnt, while e_t and η_t are the regression errors (to be minimized during the learning procedure). The coefficients in z_t are also called the latent variables in the PLS representation (6): they aim at summarizing the cross-information between x_t and y_t. l_v is defined as the size of z_t, i.e. it corresponds to the number of latent variables used in (6).

When processing a new validation image, system (6) is used to evaluate the y_t associated to the image. Let $\hat{y}_t$ be the estimated output computed by means of (6) and y_t the correct output (ground truth). Then, the root mean square error between $\hat{y}_t$ and y_t is computed to evaluate the system performance.

The reader is referred to Geladi and Kowalski [1986] for a more detailed description of PLS and its applications.

4. RESULTS AND DISCUSSIONS

In this section the proposed procedure for fiber diameter distribution estimation is tested on a data set of 62 membrane images.

For comparison, MIA and model (6) are applied for different values of the neighborhood size d, the number of principal components, n, used in MIA, and the number of latent variables, l_v, in system (6). In particular, such parameter values vary among the following sets:

$$\begin{aligned} d &= \{1, 3, 5, 7, 9, 11, 13, 15, 17, 19\} \ , \\ n &= \{2, 5, 9\} \ , \\ l_v &= \{2, 4, 6, 8, 10, 12, 14, 16, 18, 20, 22\} \ . \end{aligned}$$

Then, for each choice of the parameters the following learning and cross-validation procedure is used:

- The data set is partitioned in 6 groups of 10 images, and a 7th group containing the remaining 2 images.
- Each of the first 6 groups is iteratively selected: at each step of iteration the selected group is used as validation set, while the 52 non-selected images are used for learning the parameter values in MIA and in model (6). A normalized estimation error (NE) between the estimated and the ground truth diameter distribution values is computed on the validation set at each step of iteration, e.g. at step 1 the validation set is formed by the first 10 images, and their normalized error is computed as:
$$\text{NE}_1 = \sum_{t=1}^{10} \sum_{h=1}^{19} \left| \frac{\hat{y}_t(h) - y_t(h)}{190 \cdot y_t(h)} \right| \ .$$
- The validation results are computed as the mean values of those obtained in the six iterations, i.e. $\text{NE} = \frac{1}{6} \sum_{h=1}^{6} \text{NE}_h$.

The results of the described validation procedure are summarized in Table 4. Notice that, for the sake of readability of the table, for each value of d only the best choice for the parameters n and l_v is reported, i.e. only the model which achieves the best NE performance.

Table 1. Fiber diameter distribution estimation

d	n	l_v	NE [%]
1	9	8	6.67
3	5	8	6.59
5	2	8	6.68
7	5	20	5.14
9	5	22	4.78
11	9	2	6.86
13	5	2	7.18
15	9	2	7.22
17	5	14	6.83
19	5	22	5.34

Furthermore, Figure 4 shows the comparison, on the test image of Figure 1, between the ground truth fiber diameter cumulative distribution (measured with the method described in Tomba et al. [2010]) and the estimated ones. Similarly, Figure 5 shows the cumulative distribution estimation error. In both the figures are reported the results obtained with a small, $d = 1$, and an optimal, $d = 9$, size of the neighborhood. The corresponding values of n and l_v are as in Table 4.

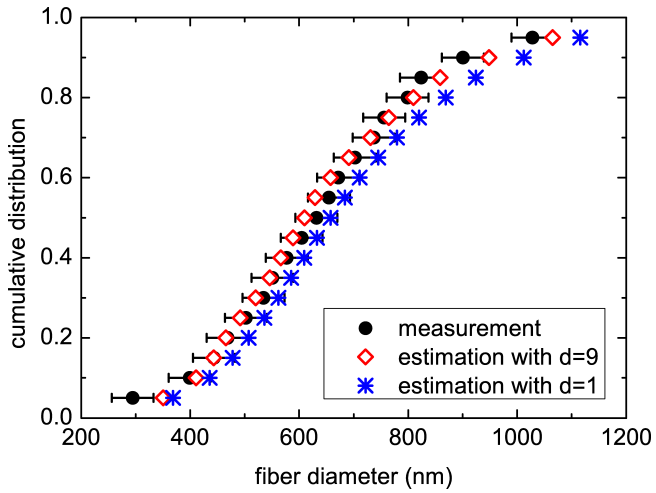

Fig. 4. Example of fiber diameter distribution estimation. Black spot: measured (ground truth) cumulative distribution. Blue star: estimated cumulative distribution with $d = 1$. Red diamond: estimated cumulative distribution with $d = 9$. The values of the other parameters are as in Table 4.

Some observations are now in order. the results in Table 4 show that considering a larger neighborhood can significantly increase the system performance, at least in this case study. Specifically, the best NE reached with $d = 1$ is 6.67%, while the best NE among all the considered choices of the parameters is 4.78%, with $d = 9$. Thus, the performance improvement with respect to the $d = 1$ case is of approximatively $(6.67 - 4.78)/6.67 = 28.3\%$.

From a computational point of view, the main advantages of the improved MIA approach are the much lower memory

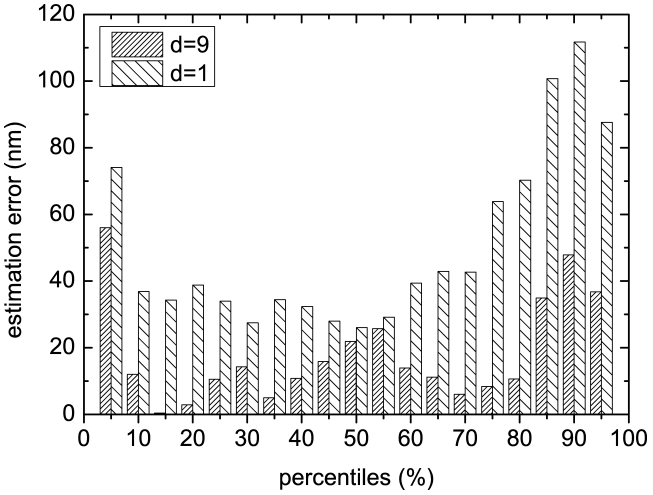

Fig. 5. Example of fiber diameter distribution estimation: difference between ground truth cumulative distribution and estimated ones with $d = 1$ and $d = 9$. The values of the other parameters are as in Table 4.

requirements and its computational efficiency, which allow to compute texture features also at quite large spatial distances.

The computational complexity of standard MIA is determined by the use of the SVD [2] and its $O(rcd^4)$, where usually $r \approx c$ and $c \gg d$, i.e. in the simulations of this section $c \approx 1000$, $d < 20$.

In the improved MIA case, the computational cost, $O(rc\log(\max(r,c)) + d^6 + rcnd^2)$, is decomposed in three terms, due to, respectively, the FFT, the SVD decomposition of C and the computation of X. For typical values of the parameters the first two terms are negligible, and the complexity of the improved MIA approach, $O(rcnd^2)$, results to be much lower than the standard MIA case.

Similar considerations can be repeated also for the memory requirements.

A practical confirmation of the above observations is provided by the simulations performed in the case study presented in this section: using standard MIA the simulations were limited to $d \leq 2$ because of out of memory errors [3] for $d \geq 3$, while it was possible to apply the improved MIA approach even with $d = 30$. Larger values of d were not tested on the improved MIA approach for several reasons: first, because the boundary value of feasibility depends on the particular machine which is used. Furthermore, changes in r and c may reflect in possible changes in such boundary value. Finally, $d = 30$ corresponds to a neighborhood of size 61×61 pixels^2 which should be sufficient for almost all the possible applications.

Finally, notice that, in this case study, the optimum neighborhood width is 19 pixels (determined by $d = 9$ in Table 4), which approximatively corresponds to the mean fiber width (in pixels). This observation suggests that the optimal size of the spatial neighborhood in the MIA is

[2] The computational complexity for computing the SVD of $h \times w$ matrix is approximatively $O(hw^2)$, where $h \geq w$.
[3] Using Matlab on a computer with 4GBytes RAM.

related to the size of the texture features in the considered images.

Then, the rationale is that the use of a large neighborhood is convenient when the texture features are quite large; conversely when the texture characteristics are very local a small d should be considered in MIA. This consideration is in accordance with the suggestion provided in Bharati et al. [2004] (i.e. using $d = 1$) where texture spatial features are typically limited to the size of few pixels.

5. CONCLUSIONS

In this paper a recently proposed multivariate image analysis techniques has been improved. This technique has been used in several applications for extracting image texture characteristics and for image denoising. In spite of the quite large range of applications in which it has been applied, due computational reasons its use has been limited to the analysis of only very local texture characteristics, i.e. very small neighborhood size, d typically lower or equal than 2.

The revised algorithm proposed here extends the use of the MIA technique allowing the choice of quite large neighborhood sizes. This has been possible by reformulating the MIA algorithm in a more efficient way (both computationally and from the memory requirements point of view).

The proposed improved MIA approach has been applied to the problem of estimating nanofiber diameter distributions. The results in this case study prove that an increase in the spatial neighborhood size for the texture statistical characterization can significantly improve the diameter estimation performances.

ACKNOWLEDGEMENTS

The authors would like to gratefully acknowledge Prof. M. Modesti (University of Padova, Italy) for providing the set of images used in this work. P. F. and M. B. gratefully acknowledge the financial support granted to this work by the University of Padova under Project CPDR088921-2008 on "Innovative techniques for multivariate and multiscale monitoring of quality in the industrial production of high added-value products".

REFERENCES

M.H. Bharati, J.J. Liu, and J.F. MacGregor. Image texture analysis: methods and comparison. *Chemometrics and Intelligent Laboratory Systems*, 72:57–71, 2004.

P. Facco, F. Bezzo, M. Barolo, R. Mukherjee, and J.A. Romagnoli. Monitoring roughness and edge shape on semiconductors through multiresolution and multivariate image analysis. *AIChE Journal*, 55:1147–1160, 2009.

P. Facco, E. Tomba, M. Roso, M. Modesti, F. Bezzo, and M. Barolo. Automatic characterization of nanofiber assemblies by image texture analysis. *Chemometrics and Intelligent Laboratory Systems*, 103:66–75, 2010.

S. Garcia-Munoz and D.S. Gierer. Coating uniformity assessment for colored immediate release tablets using multivariate image analysis. *International Journal of Pharmaceutics*, 395:104–113, 2010.

P. Geladi and B.R. Kowalski. Partial least-squares regression: a tutorial. *Analytica Chimica Acta*, 185:1–17, 1986.

R.A. Horn and C.R. Johnson. *Matrix Analysis*. Cambridge University Press, 1985.

M. Idrissa and M. Acheroy. Texture classification using gabor filters. *Pattern Recognition Letters*, 23(9):1095–1102, 2002.

J.E. Jackson. *A user's guide to principal components*. John Wiley and Sons Inc., New York (U.S.A.), 1991.

S. Kucheryavski, I. Belyaev, and S. Fominykh. Estimation of age in forensic medicine using multivariate approach to image analysis. *Chemometrics and Intelligent Laboratory Systems*, 97:39–45, 2009.

J.J. Liu and J.F. MacGregor. On the extraction of spectral and spatial information from images. *Chemometrics and Intelligent Laboratory Systems*, 85:119–130, 2007.

J.J. Liu, M.H. Bharati, K.G. Dunn, and J.F. MacGregor. Automatic masking in multivariate image analysis using support vector machines. *Chemometrics and Intelligent Laboratory Systems*, 79:42–54, 2005a.

J.J. Liu, J.F. MacGregor, C. Duchesne, and G. Bartolacci. Flotation froth monitoring using multiresolutional multivariate image analysis. *Minerals Engineering*, 18:65–76, 2005b.

S. Mallat. *A wavelet tour of signal processing*. Academic Press, 1999.

A.V. Oppenheim and R.W. Schafer. *Digital signal processing*. Prentice-Hall, Englewood Cliffs, NJ., 1975.

J.M. Prats-Montalban and A. Ferrer. Integration of colour and textural information in multivariate image analysis: defect detection and classification issues. *Journal of Chemometrics*, 21:10–23, 2007.

M.S. Reis and A. Bauer. Wavelet texture analysis of on-line acquired images for paper formation assessment and monitoring. *Chemometrics and Intelligent Laboratory Systems*, 95:129–137, 2009.

M. Roso, S. Sundarrajan, D. Pliszka, S. Ramakrishna, and M. Modesti. Multifunctional membranes based on spinning technologies: the sinergy of nanofibers and nanoparticles. *Nanotechnology*, 19:1–6, 2008.

G.C. Rutledge and S.V. Fridrikh. Formation of fibers by electrospinning. *Advanced Drug Delivery Reviews*, 59: 1384–1391, 2007.

E. Tomba, P. Facco, M. Roso, M. Modesti, F. Bezzo, and M. Barolo. Artificial vision system for the automatic measurement of inter-fiber pore characteristics and fiber diameter distribution in nanofiber assemblies. *Industrial and Engineering Chemistry Research*, 49:2957–2968, 2010.